DOI: 10.1021/ma901251y

Macromolecules
ARTICLE

Tuning the Free Volume Cavities of Polyimide Membranes via the Construction of Pseudo-Interpenetrating Networks for Enhanced Gas Separation Performance

Bee Ting Low,[†] Tai Shung Chung,*[,†] Hongmin Chen,[‡] Yan-Ching Jean,[‡] and Kumari Pallathadka Pramoda[§]

[†]*Department of Chemical and Biomolecular Engineering, National University of Singapore, 10 Kent Ridge Crescent, Singapore 117602,* [‡]*Department of Chemistry, University of Missouri-Kansas City, Kansas City, Missouri 64110, and* [§]*Institute of Materials Research and Engineering, 3 Research Link Singapore 117602*

Received June 11, 2009; Revised Manuscript Received August 11, 2009

ABSTRACT: A novel synthetic strategy to fine-tune the cavity size and free volume distribution of polyimide membranes via the formation of homogeneous pseudo-interpenetrating polymer networks (IPN) is explored in this study. The transformation in the free volume characteristics of the pseudo-IPN can be effectively exploited for achieving enhanced gas transport properties. The construction of the pseudo-IPNs entails the in situ polymerization of azido-containing monomers with multireactive sites within rigid polyimide molecular scaffolds. The intrinsic free volume of the host polyimide and the dimensions of the azido-containing monomer predominantly influence the mean cavity size of the semi-IPN. The pseudo-IPNs assembled using fluorinated polyimides and 2,6-bis(4-azidobenzylidene)-4-methylcyclohexanone (azide) display improved CO_2/CH_4 and H_2/N_2 separation performance. The alterations in the gas permeability and gas pair permselectivity of the semi-IPNs are adequately mapped to the variation in the free volume distributions characterized by the positron annihilation lifetime spectroscopy. Depending on the functionalities of the host polyimides, chemical cross-links are formed between the azide network and the preformed linear polyimide. The chemical bridges in conjunction with the interpenetrating network restrict the mobility of the polymer chains and suppress CO_2-induced plasticization.

1. Introduction

The implementation and establishment of the membrane technology for gas separation are dependent on the constructive integration of membrane material advancement, membrane configuration and module design, and process optimization.[1−4] Indeed, the development of high performance membrane materials is the vital aspect among these considerations.[1,5] Polymers are attractive candidates for membrane fabrication due to the ease of processability, good physiochemical properties and low production costs.[6−9] In order to satisfy the demands from diverse applications, the properties of polymers can be tailored by various approaches. The molecular architecture of polymers by the permutations of numerous monomers represents one of the conventional approaches by membrane scientists to accomplish this goal.[8,9] Glassy polyimides have been extensively studied as promising materials for gas separation membranes and the molecular tailoring method has been particularly effective for enhancing the CO_2/CH_4 separation performance.[10−13] The integration of soft rubbery segments with hard glassy segments in the form of block copolymers has been investigated and these materials display recommendable CO_2/N_2 and CO_2/H_2 separation properties.[14,15] The molecular design technique creates novel polymers with robust separation performance and excellent intrinsic properties but is less attractive from the economical aspect as the approach is time-consuming and incurs substantial costs.

The modification of existing polymers is an alternative route for functionalizing either the selective layer or the bulk of the membrane. This is realizable by various techniques including chemical modification, thermal annealing, ion-beam irradiation and plasma treatment.[16−26] Hayes proposed a diamine modification approach as a post-treatment for polyimide membranes.[16] This technique was comprehensively examined by Chung and co-workers for enhancing the CO_2/CH_4 and H_2/CO_2 separation performance of polyimide membranes.[17−19] The simplicity and applicability to various polyimides and asymmetric hollow fiber membranes are the merits of this approach but the reversible nature of the reaction at high temperatures constitutes a major concern.[18,20] Wind et al. employed diol cross-linking at elevated temperatures for polyimides containing carboxylic acid groups to improve CO_2/CH_4 selectivity and to suppress CO_2-induced plasticization of the dense membrane.[21,22] The diol cross-linking technique has been implemented on hollow fiber membranes by Omole et al. In their study, the diol-grafted polyimide is used for fabricating the hollow fibers via phase inversion and the subsequent thermal annealing of the membrane leads to the formation of diol cross-links.[23] However, the diol cross-linking approach is only applicable for polyimides containing carboxylic acid groups. Bromination, sulfonation and metal-ions exchange are other means to chemically modify polymers.[24,25] Despite the potential use of ion-beam irradiation and plasma treatment in altering the gas transport properties, the high cost and difficulty in obtaining uniform modification may limit the industrial application of this technique. Polymer modification is simple and may produce significant changes in the properties of the resultant organic matter. However, the long-term performance and stability of the membranes may become questionable when subjected to aggressive feeds and harsh operating conditions.

Polymer blending is a viable approach which may synergistically combine the merits of different materials.[27−31] Generally,

*Corresponding author. E-mail: chencts@nus.edu.sg. Fax: (65)-67791936.

 Published on Web 08/19/2009

polymer blends display varying degrees of miscibility and homogeneous blends are preferred for membrane fabrication since the uniformity is a prerequisite for stable and reliable membrane performance.[27−31] The resultant polymer blends may exhibit exceptional properties that supersede the respective native polymers. Maeda and Paul studied the use of poly(phenylene oxide)/polysulfone blends in gas separation and for specific blend compositions, the resultant CO_2/CH_4 selectivity exceeds that of the pure component polymers.[28] Bos et al. developed Matrimid/P84 blend membranes with anti-CO_2 plasticization characteristics and good CO_2/CH_4 separation performance.[30] The advantages of polymer blending are simplicity, reproducibility and relatively short development time since it utilizes the existing polymer database. Nevertheless, one severe deficiency of polymer blending is the issue of component miscibility. In fact, there is limited availability of polymer pairs which are compatible with each other and most blends exhibit phase separation at certain compositions.

Interpenetrating polymer network (IPN) is a refinement of a linear polymer blend where two different polymer networks physically intermingle with each other in the same spatial region without chemical bonds between them.[32−38] In distinction to a linear polymer blend system where coarse phase separation frequently occurs, the physical interconnections present in an IPN greatly enhance the degree of polymer compatibility. A network polymer that encompasses a linear polymer gives rise to a pseudo- or semi-IPN.[32] A pseudo-IPN is produced either by (1) the polymerization of the precursors of a branched polymer in the presence of a preformed linear polymer or (2) the formation of a straight-chain polymer within a pre-existing network. One shortcoming of the aforementioned methods for producing pseudo-IPNs is the extractability of the linear component from the composite material.[32] Therefore, attempts were made to immoblize the linear component within the semi-IPN via chemical bonds with the networked polymer.[32,34] This results in interconnected pseudo-IPNs and it has been shown that such intralinkages greatly influence the structural properties of the resultant materials. IPNs are novel and versatile composite materials for many applications, including their prospective use as a barrier material for gas separation. The interconnections between the constituent polymers in an IPN possibly reduce the undesirable swelling effects of polymers by highly condensable gases. This favorable characteristic of IPNs may be exploited in natural gas purification which involves plasticizing components like CO_2 and H_2O. Despite the merits of IPN materials and their potential use in membrane gas separation, the studies devoted to this research area are rather limited.[39−44]

In this article, a synthetic strategy for the construction of pseudo-IPNs by the polymerization of multifunctional azido-containing monomers within preformed linear polyimide frameworks is explored. Considering the ability of 2,6-bis(4-azidobenzylidene)-4-methylcyclohexanone (azide) to react spontaneously in the presence of heat or UV light and its rigid conjugated structure, it was chosen as the monomer for creating the network polymer.[40] Here, the network polymer formed by the azide monomer is termed poly(azide). Polyimide has not been extensively investigated as a component for forming IPN materials. In view of its superior intrinsic properties, it is worthwhile to explore its application in this area. Hence, fluorinated polyimides, poly(1,5-naphthalene-2,2′-bis(3,4-phthalic) hexafluoropropane) diimide (6FDA−NDA) and poly(2,3,5,6-phenylene-2,2′-bis(3,4-carboxylphenyl) hexafluoropropane) diimide (6FDA−TMPDA), with high free volume and rigidity were selected as the host polymers for creating the pseudo-IPNs. The high free volume provides the opportunity to manipulate the cavity distribution of the resultant composite material upon the formation of the branched poly(azide). The anticipated change in the free volume distribution is likely to impact the gas transport properties of the membranes. Aromatic polyimides with limited chain mobility provide the ideal rigid frameworks for the polymerization of azide. A firm molecular scaffold is essential to minimize the likelihood of generating a phase-separated semi-IPN. This is attributed to the fact that when the azide monomers react to form a polymer network, there is a tendency for the branched macromolecule to push apart the existing linear polymer chains. Hence, the susceptibility of the linear prepolymers to the molecular force results in the formation of undesirable phase separated domains.[33] 6FDA−based polyimide/azide membranes with varying compositions are fabricated and characterized. The chemical reactions occurring during the thermal treatment are investigated in order to elucidate and validate the pseudo-IPNs formation. Depending on the functionalities of the host polymer, chemical cross-links may be formed between the linear and the branched polymer, resulting in an interconnected pseudo-IPN. The homogeneity and thermal properties of the semi-IPN membranes are analyzed, and the changes in the free volume and free volume distribution in relation to the gas transport properties of the composite films are discussed. The CO_2/CH_4 separation performance and CO_2−induced plasticization behavior of these semi-IPN membranes are highlighted.

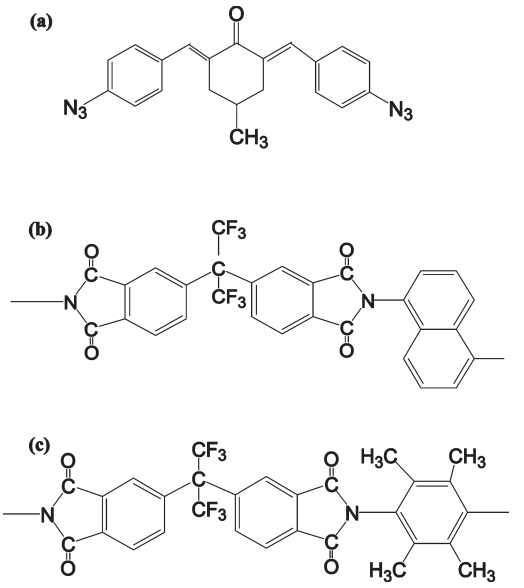

Figure 1. Chemical structures of (a) 2,6-Bis(4-azidobenzylidene)-4-methylcyclohexanone, (b) 6FDA−NDA polyimide, and (c) 6FDA−TMPDA polyimide.

2. Experimental Section

2.1. Materials. The working polyimides were synthesized via the chemical imidization approach. The monomers 4,4′-(hexafluoroisopropylidene)diphthalic anhydride (6FDA) and 1,5-naphthalenediamine (NDA) were sublimated under vacuum prior to use. 2,3,5,6-tetramethyl-1,4-phenylenediamine (TMPDA) was purified by recrystallization in methanol at 55 °C. 6FDA, NDA, and TMPDA were purchased from Clariant (Germany), Acros Organics, and Sigma-Aldrich, respectively. 2,6-bis(4-azidobenzylidene)-4-methylcyclohexanone (azide) from Sigma-Aldrich was used without further purification. The chemical structure of azide is depicted in Figure 1a. *N*-Methyl-2-pyrrolidone (NMP) from Merck was purified via vacuum distillation before use.

Equimolar amounts of dianhydride and diamines were dissolved in NMP under nitrogen atmosphere to form a viscous solution of poly(amic acid). The total solid concentration was 20% by weight. 3-picoline and acetic anhydride (molar ratio of 1:4)

Table 1. Mass Compositions of Polyimide/Azide Casting Solutions

polyimide/azide composition (wt %: wt %)	mass of polyimide[a] (g)	mass of solvent[b] (g)	mass of azide (g)
100:0	1.149	21.83	0
90:10			0.128
70:30			0.492
50:50			1.149

[a] The polymer concentration in the solvent is 5 wt % and the azide loading in the polymer varied from 0 to 50 wt %. [b] The solvents used for 6FDA−NDA and 6FDA−TMPDA polyimides are DMF and DCM, respectively.

were added to form the polyimide. The polyimide solution was precipitated in methanol and dried under vacuum at 120 °C prior to use. A detailed description of the polymer synthesis can be obtained elsewhere.[19] The chemical structures of 6FDA−NDA and 6FDA−TMPDA are shown in Figures 1(b) and 1(c). Dimethylformamide (DMF) and dichloromethane (DCM) were used as solvents for 6FDA−NDA and 6FDA−TMPDA, respectively.

2.2. Dense Membrane Fabrication. To prepare the film casting solution, the azide monomer was first dissolved in the solvent and stirred for 1 h. Subsequently, the polyimide was added to the solution and stirred overnight. The polymer concentration in the solvent is 5 wt % while the azide loading in the polymer varied from 0 to 50 wt %. Table 1 shows the mass of the respective chemical species constituting the casting solutions. The solution was filtered using 1.0 μm PTFE membrane before ring casting onto a Si wafer plate. The casting of 6FDA−NDA/azide and 6FDA−TMPDA/azide films was carried out at 55 and 25 °C, respectively. The casting temperature was selected based on the volatility of the solvent and to allow slow solvent evaporation for forming the polymer film. After approximately 5 days, most of the solvent has evaporated, leaving behind the nascent film. Further heat treatment of the 6FDA−based polyimide/azide films was conducted under vacuum as follows: (1) hold at 60 °C for 24 h, (2) increase to 250 at 12 °C/20 min, (3) hold at 250 °C for 24 h, and (4) natural cooling.

2.3. Characterization. The chemical functionalities of the polymeric membranes were monitored by the attenuated total reflectance (ATR) mode using a Shimadzu FTIR 8400 spectrometer over the range 650−2000 cm^{-1}. As the azide monomer is in powder form, the sample was diluted with KBr (i.e., 1 mg of azide with 100 mg of KBr) and compressed into a pellet which was analyzed by the direct transmittance mode using the same scanning range. The number of scans for each sample was 32.

To examine the extent of chemical reactions occurring at different temperatures, the nascent films were subjected to thermal annealing (i.e., heating rate of 0.6 °C/min from 25 °C to the desired baking temperature, hold for 2 h followed by natural cooling). The final annealing temperatures were 55, 80, 100, 150, 200, and 250 °C. The gel content of these thermally treated films was determined by immersing the films in the original solvents (i.e., DMF for 6FDA−NDA/azide films and DCM for 6FDA−TMPDA/azide films) for 5 days. DMF and DCM are considered as relatively mild solvents. Therefore, a much stronger solvent, NMP was used for analyzing the extractability of 6FDA−TMPDA/azide (70−30) films annealed at different temperatures. The extraction was performed at an elevated temperature of 180 °C over 5 days. The effect of using different solvent and extraction conditions on the gel content will be presented. The remaining insoluble portions of the membranes were dried under vacuum at 100 °C for 24 h to remove the residual solvent before weighing. The gel content was calculated by eq 1.

$$\%\ \text{gel content} = M_1/M_0 \times 100\% \quad (1)$$

where M_1 and M_0 are the mass of the insoluble fraction and the original mass of the film, respectively.

The molecular weights of the 6FDA−NDA host polyimide and the soluble portions of 6FDA−NDA/azide films were determined using gel permeation chromatography (GPC). The Waters GPC system comprises a Waters 2414 refractive index detector and a Waters 1515 isocratic HPLC pump. The system was allowed to reach stable equilibrium before analysis and polystyrene standards were used for calibration. HPLC grade DMF was used as the mobile phase. The flow rate of the mobile phase was 1 mL/min and the injection volume was 50 μL. The testing temperature was set at 25 °C.

The glass transition temperatures (T_g) of polymer films were characterized by differential scanning calorimetry (DSC) using a Mettler Toledo DSC 822 at a heating rate of 20 °C/min from 50 to 450 °C under nitrogen purge of 30 mL/min. Two heating-and-cooling cycles were performed for each sample in order to remove the thermal history of the film. The T_g was obtained from the second heating curve. Dynamic mechanical analysis (DMA) measurements were carried out for the pseudo-IPNs with a TA Instruments DMA 2980 operating in a tension mode. The testing samples are 35 mm by 6 mm and the experiments were performed at a 1 Hz frequency and a heating rate of 3 °C min^{-1} from 30 to 480 °C. The thermal decomposition behaviors of the membranes were analyzed by thermal gravimetric analysis (TGA) using a TGA 2050 thermogravimetric analyzer (TA Instruments) at a heating rate of 20 °C/min from 50 to 800 °C under nitrogen purge. The temperature at 5% weight loss is taken as the decomposition temperature of the material.

The changes in the intersegmental properties of polymeric membranes were investigated using an X-ray diffractor (XRD) Bruker, D8 series, GADDS (general area detector diffraction system). A Cu X-ray source of wavelength 1.54 Å was used. The average *d*-spacing was determined based on the Bragg's law as shown in eq 2

$$n\lambda = 2d \sin\theta \quad (2)$$

where n is an integer, λ denotes the X-ray wavelength, d represents the intersegmental spacing between two polymer chains and θ indicates the diffraction angle.

The positron annihilation lifetimes of the host polyimides and the pseudo IPNs were obtained using positron annihilation lifetime spectroscopy (PALS). The positron source of approximately 25 μCi of ^{22}Na was sealed by Kapton films and then sandwiched between layers of polymeric membranes. The ^{22}Na source/polymer films assembly was wrapped in Al foil and clamped in between two sets of plastic scintillators and photomultipliers which are aligned facing to each other. The positrons emitted from the ^{22}Na source were absorbed by the polymer samples and were eventually annihilated. The lifetime of each positron terminates with the emission of two 0.511 MeV γ-rays. The generation of a 1.275 MeV γ-ray marks the incipient creation of the positron. The time difference between the detection of the start and end γ-rays were recorded using a fast−fast coincidence timing system. The resolution of the positron annihilation lifetime spectrometer was determined by measuring ^{60}Co and the full width at half-maximum (fwhm) of the spectrum was 300 ps. All the lifetime spectra were binned into 1024 channels, with a channel width of 51 ps. The analyses were conducted at 25 °C and two million counts were collected in about 2 h for each PAL spectrum. A detailed description of the PALS can be obtained elsewhere.[45−49]

2.5. Gas Permeation Tests. The gas transport properties of the dense membranes were tested in the order He, H_2, O_2, N_2, CH_4, and CO_2. The pure gas measurements were done using a variable-pressure constant-volume gas permeation cell. A detailed description of the permeation cell setup and testing procedures can be obtained elsewhere.[50] H_2 permeation was conducted at 3.5 atm while CO_2 was tested at 3.5 and 10 atm.

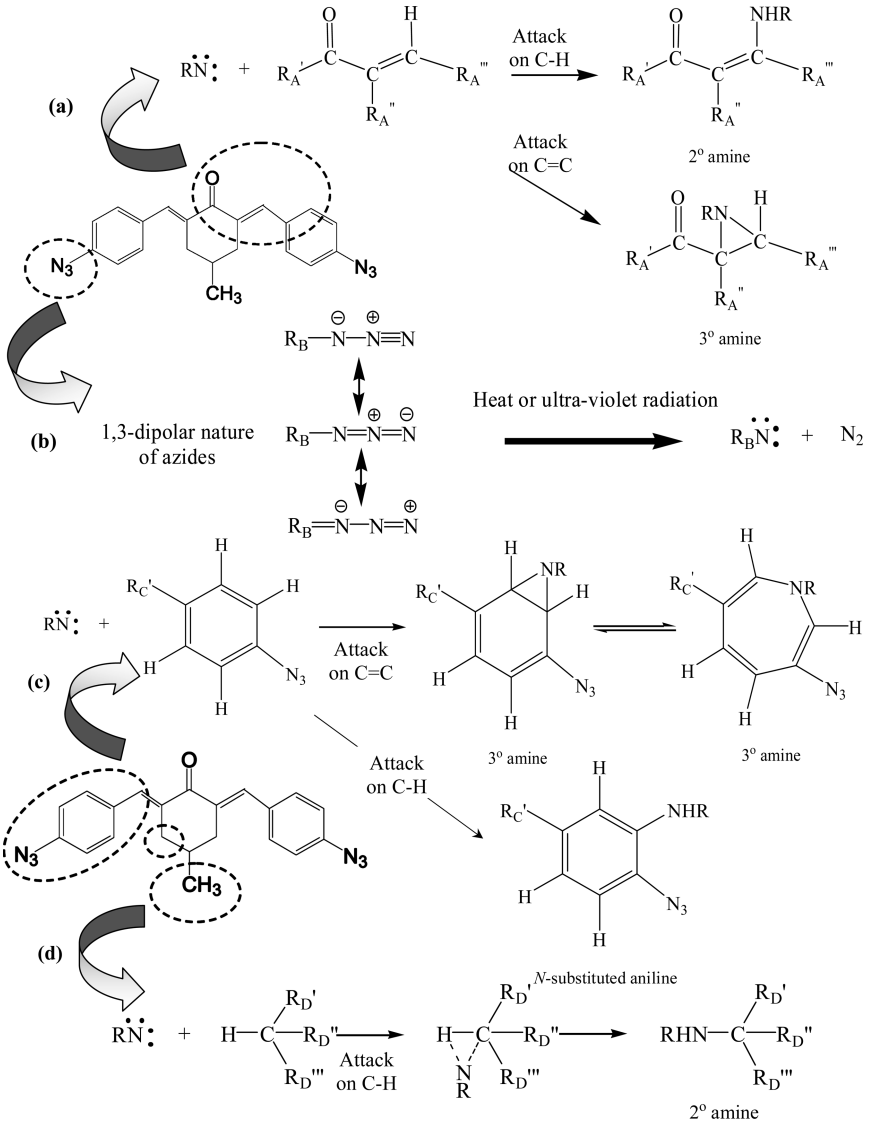

Figure 2. (a) Reactions of nitrene with alkene C=C and C−H bonds, (b) generation of nitrene from azide, (c) reactions of nitrene with benzene C=C and C−H bonds, and (d) reaction of nitrene with alkyl C−H bonds.

The remaining gases were tested at 10 atm. The operating temperature was 35 °C. To investigate the CO_2-induced plasticization behavior of the films, the testing pressure was intermittently ramped from 2 to 30 atm (i.e., 29.4 to 441 psia) and pure CO_2 was used. The rate of pressure increase (dp/dt) at steady state was used for the calculation of gas permeability according to eq 3 and the ideal permselectivity of gas A to gas B, α was evaluated using eq 4

$$P = \frac{273 \times 10^{10}}{760} \frac{VL}{AT\left(p_2 \times \frac{76}{14.7}\right)} \left(\frac{dp}{dt}\right) \tag{3}$$

where P is the gas permeability of a membrane in barrer (1 barrer $= 1 \times 10^{-10}$ cm^3 (STP) cm/cm^2 s cmHg), V is the volume of the downstream chamber (cm^3), A refers to the effective membrane area (cm^2), l is the membrane thickness (cm), T is the operating temperature (K) and the upstream pressure is given by p_2 (psia).

$$\alpha = \frac{P_A}{P_B} \tag{4}$$

where P_A and P_B are the gas permeabilities for A and B, respectively.

Mixed gas permeation tests were conducted for the intrinsic polyimide films and the pseudo-IPN membranes which exhibited promising ideal CO_2/CH_4 permselectivity. Binary gas tests using 90% CO_2 and 10% CH_4 feed at 10, 20, and 30 atm were tested. The temperature was 35 °C. A detailed description of the facility used for mixed gas permeation tests has been previously reported.[50] The gas permeability was determined using eqs 5 and 6 as follows:

$$P_{CO_2} = \frac{273 \times 10^{10}}{760} \frac{y_{CO_2} VL}{AT\left(\frac{76}{14.7}\right)(x_{CO_2} p_2)} \left(\frac{dp}{dt}\right) \tag{5}$$

$$P_{CH_4} = \frac{273 \times 10^{10}}{760} \frac{y_{CH_4} VL}{AT\left(\frac{76}{14.7}\right)(x_{CH_4} p_2)} \left(\frac{dp}{dt}\right) \tag{6}$$

where P_{CO_2} and P_{CH_4} are the permeabilities (barrer) of CO_2 and CH_4 respectively. p_2 is the upstream feed gas pressure (psia) and p_1 represents the downstream permeate gas pressure (psia). x and y refer to the gas molar fraction in the feed and the permeate accordingly (%). Subsequently, the mixed gas selectivity can be simplified into the calculating equation as described in eq 4 due to the negligible downstream pressure.

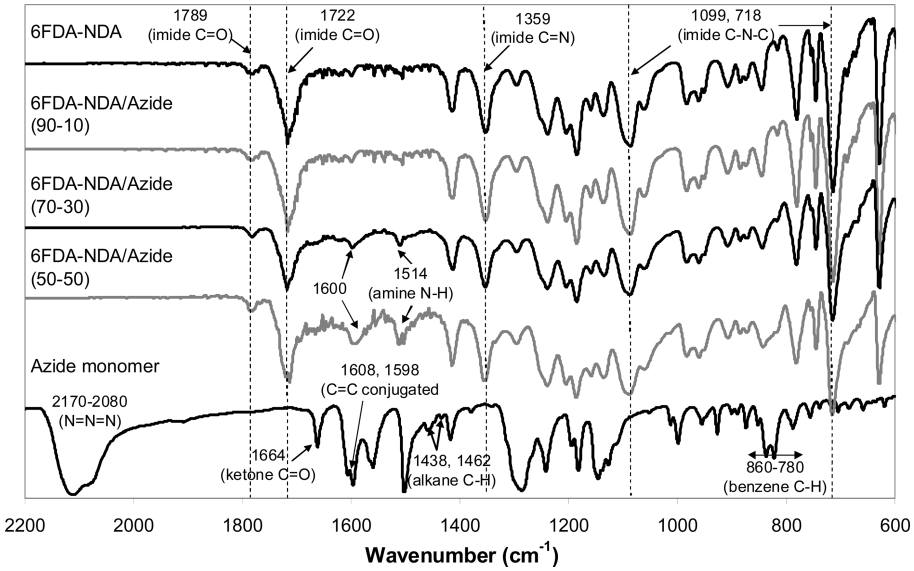

Figure 3. FTIR spectra of 6FDA−NDA, 6FDA−NDA/azide films and azide monomer.

3. Results and Discussion

3.1. Chemical Reactions of 2,6-Bis(4-azidobenzylidene)-4-methylcyclohexanone (Azide). In this study, the chosen azido-containing monomer for creating the network polymer is of complicated chemical nature due to the presence of various reactive functional groups. This section aims to elucidate the relative reactivity of different functional groups. The azido group, N_3 is a linear 1,3-dipolar structure which easily forms nitrene in the presence of heat or ultraviolet radiation. Nitrenes are highly reactive, short-lived nitrogen intermediates. The nitrogen atom has four nonbonded electrons which accounts for the electrophilicity of nitrene. Nitrenes are capable of insertion into C−H bonds and addition to unsaturated C−C bonds (i.e., alkenes, alkynes, and arenes).[51] Figure 2 shows the formation of nitrene and the possible reactions of the different functional groups with the nitrene radical.

FTIR analyses were performed to verify the reactions induced by the azide monomer. Figure 3 depicts the FTIR spectra for the azide monomer and 6FDA−NDA/azide films. Referring to the spectrum for azide, the strong band in the region 2170−2080 cm^{-1} is due to the asymmetric stretching vibration of the N=N=N group.[52] The prominent peak at 1664 cm^{-1} is attributed to C=O stretching vibration of the α,β-,α',β'-diunsaturated ketone (i.e., >C=C−CO−C=C<).[52] The C=C stretching vibration of this conjugated system gives rise to a doublet at 1608 and 1598 cm^{-1}. The series of bands in the region 860−780 cm^{-1} result from the C−H out-of-plane vibrations of 1,4-disubstituted benzenes.[52] The peaks at 1438 cm^{-1} and 1462 cm^{-1} reflect the alkane C−H deformation vibrations.[52] The pristine 6FDA−NDA film exhibits two peaks at 1719 cm^{-1} and 1789 cm^{-1} which are attributed to the carbonyl group of the imide ring.[19] The characteristic peak at 1356 cm^{-1} is due to the C−N stretch of the imide group while the peak at 1095 cm^{-1} is indicative of the transverse stretch of C−N−C in the imide group.[19] The peak at 716 cm^{-1} is due to the out-of-plane bending of C−N−C in the imide group.[19]

With the incorporation of azide to the polyimide host, the characteristic peak of the N=N=N group is not observed. This provides evidence for the formation of nitrene (Figure 2b) and its subsequent reaction, i.e., polymerization of azide. With reference to Figure 3, the addition of azide results in the appearance of two strong peaks at 1600 and 1514 cm^{-1}. The transformation of the original doublet at 1608 and 1598 cm^{-1} of the azide monomer to the single peak at 1600 cm^{-1} for the 6FDA−NDA/azide films indicates some changes in the chemical functionalities. The peak at 1600 cm^{-1} may be attributed to the presence of α,β-unsaturated ketones with a β-amino group (Figure 2a, reaction with C−H bond).[52] This implies that the C−H bond at the β-position of the unsaturated ketone is susceptible to electrophilic attacks by nitrenes. The intramolecular hydrogen bonding between the amino and ketone group accounts for the slight broadening of this peak. The peak at 1514 cm^{-1} is representative of the N−H deformation vibration of secondary amines.[52] Generally, the selectivity of C−H insertion follows the reactivity pattern of tertiary > secondary > primary C−H bonds.[51] The alkane C−H deformation vibration of the azide monomer is not observed in the composite polymeric films which support the C−H insertion of nitrenes (Figure 2, parts a and d). Conversely, the series of bands reflecting the C−H out-of-plane vibrations of the disubstituted benzenes are present with some slight changes in the peak intensity and position. This is due to the coexistence of 1,4-disubstituted phenylene rings of the poly(azide) and the naphthalene structure of the polyimide. Due to the stability of the benzene ring which comprises the highly conjugated π electrons, the C−H bonds of the phenyl group are not easily attacked by the nitrene radicals (Figure 2c). The homolytic bond dissociation energies for CH_3−H and C_6H_5−H are 435 and 460 kJ/mol, respectively.[53] This implies that the reaction between nitrene and alkyl C−H bond is more feasible from the thermodynamics aspect. The characteristic peak of tertiary amine is not observed which indicates that the cycloaddition of nitrenes to the phenyl ring and the C=C bonds has not occurred (Figure 2c). The unfavorable addition of nitrene to the C=C bonds has been reported by Kelman et al. and Shao et al. where azido-containing compounds were used to cross-link rubbery poly(1-(trimethylsilyl)-1-propyne) (PTMSP) and poly(4-methyl-2-pentyne) (PMP), respectively.[54,55] Similar results are obtained from the FTIR spectra of 6FDA−TMPDA/azide films.

On the basis of the reaction chemistry of nitrenes and the chemical functionalities of the host polyimides, the following conclusions can be made. The azide monomer with multi-reactive sites reacts with its own species to form a network polymer. The nitrene radicals react with the C−H bonds of

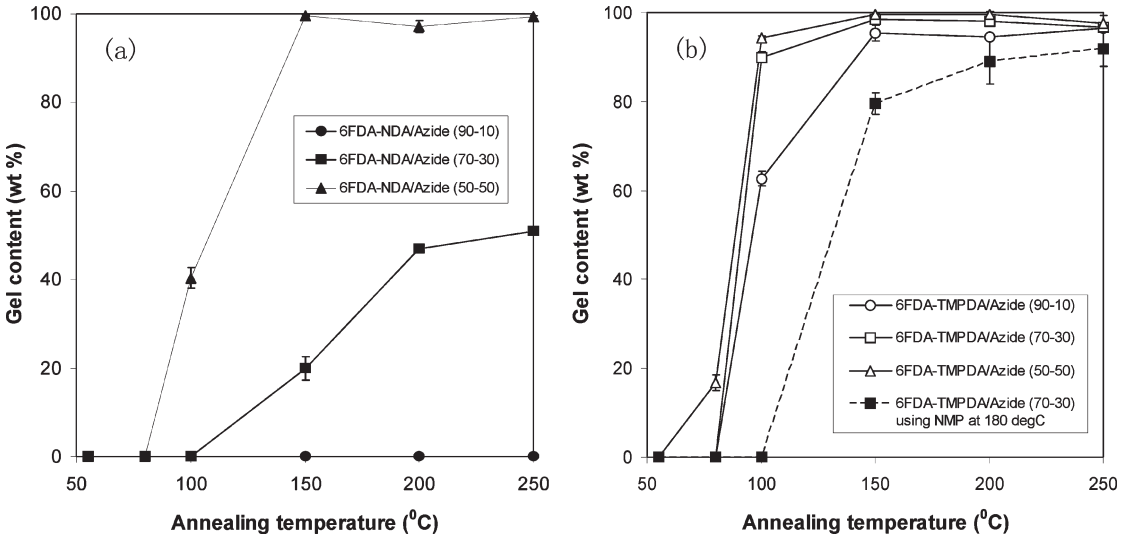

Figure 4. Gel content of (a) 6FDA−NDA/azide and (b) 6FDA−TMPDA/azide films using DMF and DCM as solvents, respectively (unless otherwise stated).

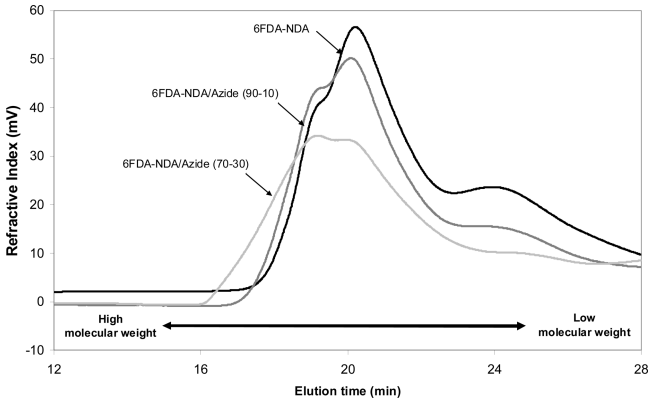

Figure 5. GPC analysis of the soluble portions of 6FDA−NDA/azide films.

the (1) α,β-unsaturated ketone, (2) $-CH_3$ substituent group, and (3) cyclohexanone structure. There is no reaction with the alkene and benzene C=C double bonds due to the presence of steric hindrance and the high stability of the conjugated system. The higher bond dissociation energy of the aromatic C−H bond makes its less vulnerable to nitrene attack. For the two host polyimides, which are considered in our study here, the main difference is the presence of $-CH_3$ groups in the diamine moieties. 6FDA−NDA does not contain any functional group that potentially reacts with azide while 6FDA−TMPDA with the methyl substituent groups may reacts with azide. Hence, depending on the chemical nature of the host polymer, the combination of polyimide and poly(azide) may results in a pseudo-IPN or an interconnected pseudo-IPN.

3.2. Validation of the Formation of a Pseudo-IPN and Interconnected Pseudo-IPN. The gel content of 6FDA−NDA/azide and 6FDA−TMPDA/azide films annealed at different temperatures is shown in Figure 4. The existence of the insoluble gel in the film reflects the formation of cross-linked networks. Comparing the gel content of the membranes with polyimide/azide composition of 90/10, 6FDA−NDA/azide films dissolve completely in the solvent regardless of the annealing temperature. Conversely, for the 6FDA−TMPDA/azide film annealed at 100 °C, the gel content is approximately 60 wt % and beyond an annealing temperature of 150 °C, the film contains more than 90 wt % of insoluble mass. The low extractability of 6FDA−TMPDA/azide films implies that these two components react with each other to form an interconnected pseudo-IPN. The high gel content of 6FDA−TMPDA/azide (70/30) film was further verified by using a stronger solvent (i.e., NMP) for extraction at 180 °C. Referring to Figure 4b, the extractability of the film in NMP is higher than in DMF. Nevertheless, a high gel content of >90% is obtained for the film that is annealed at 250 °C. On the basis of the discussion in section 3.1, the nitrene radicals react with the methyl C−H bonds of 6FDA−TMPDA to form chemical cross-links. Considering the variation in the gel content of 6FDA−TMPDA/azide films annealed at different temperatures, it can be inferred that the incipient reaction of azide falls between 80 and 100 °C.

When 6FDA−NDA is used as the host polyimide, the azide monomer solely reacts with its species to form a polymer network which physically interlocks the linear polyimide chains. At a low azide concentration of 10 wt %, the degree of interpenetration between 6FDA−NDA and the poly(azide) is limited. Thus, the resultant films dissolve completely in the solvent. Referring to Figure 4a, at higher azide concentrations, the gel content of the films increases and for the 6FDA−NDA/azide films annealed beyond a temperature of 150 °C, the gel content is >90 wt %. Hence, the extent of interpenetration between 6FDA−NDA and the in situ formed branched polymer improves significantly, which makes it is difficult for the solvent molecules to extract the linear polymer chains.

Since a significant portion of the 6FDA−NDA/azide films (90/10 and 70/30) is soluble in DMF (i.e., the solvent for 6FDA−NDA), it would be interesting to analyze the molecular weights of the soluble components. It is believed that most of the soluble mass should be contributed by the linear host polyimide which has better extractability in the solvent. The chromatograms obtained from the GPC analyses are depicted in Figure 5. For 6FDA−NDA, the shoulder peak at an elution time of approximately 24 min represents the population of the polyimide with lower molecular weights. With the addition of azide, the intensity of this shoulder peak decreases considerably. Moreover, it can be seen that the molecular weight distributions of the soluble components progressively shift toward a lower elution time (i.e., higher molecular weight) as the composition of azide increases.

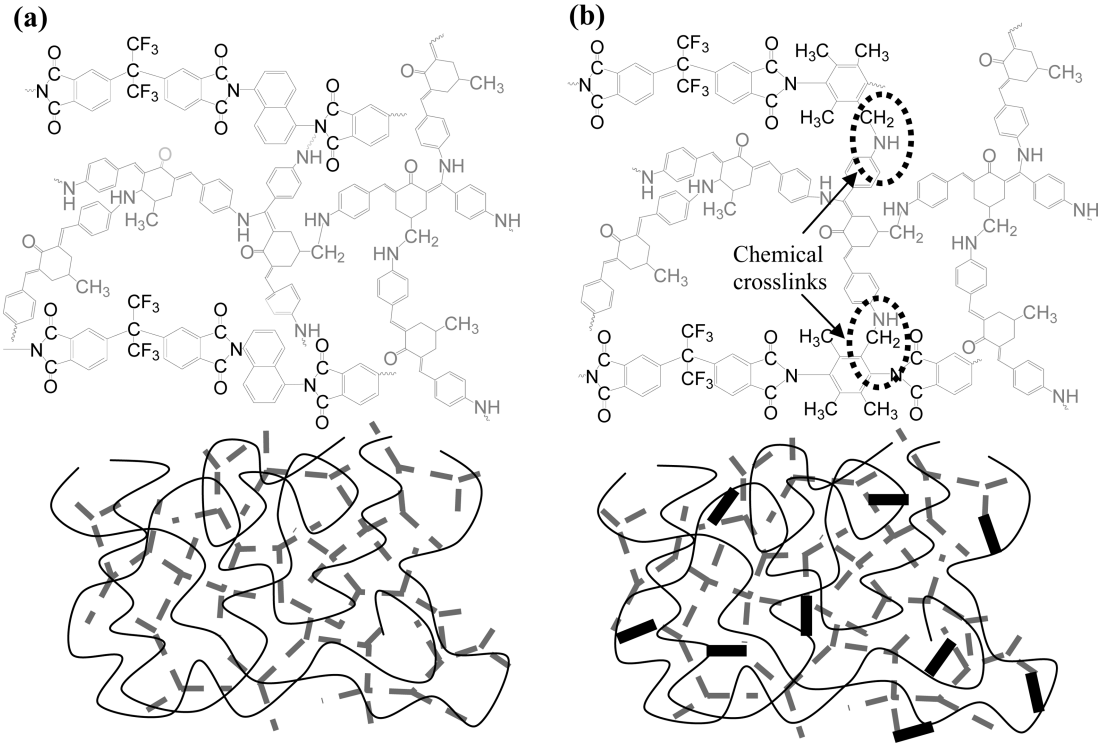

Figure 6. Schematics of (a) 6FDA−NDA/azide pseudo-IPN and (b) 6FDA−TMPDA/azide interconnected pseudo IPN: (—) host polyimide; (gray bar) poly(azide) network; (black bar) chemical cross-links.

The shift in the molecular weights distribution may be attributed to the entanglement of the linear polyimide with the poly(azide) in the solvent. At low concentrations of azide, the monomers are sparsely dispersed in the polyimide host and the resultant membrane contains tiny domains of low molecular weights poly(azide) embedded in the polyimide matrix. The small domains of poly(azide) are easily extracted together with the polyimide in the solvent and they probably remain entangled in the solution. However, as the concentration of azide increases, the size of the poly(azide) domains becomes larger. Hence, the size of the extractable poly(azide) in entanglement with the polyimide similarly increases. The insoluble portions comprise of extensive networks that physically interlock the linear chains effectively and block the access of the solvent molecules. The conclusions drawn from the FTIR, gel content and GPC analyses are 6FDA−NDA/azide forms a pseudo-IPN (Figure 6a) while 6FDA−TMPDA/azide results in an interconnected pseudo-IPN (Figure 6b).

3.3. Physical Properties of the Pseudo-IPNs. The homogeneity of a material is an important requirement for its use in all applications. For polymers that constitute two or more components, the miscibility of the components determines the overall homogeneity. The transparency of the polymer film provides a preliminary indication of the degree of miscibility, i.e., transparent films signify uniformity while opaque films indicate possible phase separation between the components. The 6FDA−NDA/azide films are completely transparent even for a high azide composition of 50 wt %. However, for 6FDA−TMPDA/azide films, at an azide content of 50 wt %, the as-cast film is opaque and heterogeneous. This suggests the likely occurrence of phase separation between the 6FDA−TMPDA and poly(azide) phases. The variation in the degree of miscibility may be attributed to the (1) difference in the solvent used, (2) film casting temperature, (3) solvent evaporation rate, and (4) chemical structure and functionalities of the host polyimides. The polymeric membranes, with the exception of 6FDA−TMPDA/azide (50:50) film which is inherently brittle, have good mechanical properties. The nonuniformity and brittleness of the 6FDA−TMPDA/azide (50:50) film limits its application and further characterization of this membrane is unnecessary.

The glass transition temperatures of the composite polymeric films were investigated and the results are shown in Figure 7, parts a and b. The presence of a single glass transition temperature is taken as a proof of the blend homogeneity for the pseudo-IPNs. For 6FDA−NDA, the incorporation of azide brings about a significant decline in the glass transition temperatures (T_g). An attempt was made to cast a pure azide solution and it was found that it has poor film forming properties. Upon solvent evaporation, only small pieces of the poly(azide) samples remain. In order to approximate the T_g of poly(azide), DSC was conducted for this sample. The poly(azide) shows a glass transition temperature of 282.6 °C. Therefore, the lower T_g of poly(azide) compared to 6FDA−NDA accounts for the decrease in T_g after the addition of azide. The pristine 6FDA−NDA polyimide exhibits a sharp transformation in the exothermic heat flow at the glass transition temperature while the change for the 6FDA−NDA/azide films occurs over a broad temperature range. The broadening of the glass transition indicates the coexistence of multiple nanodomains with varying compositions (i.e., nanohetereogeneities).[33] Each of these nanodomains has its own T_g and the resultant distribution of T_gs accounts for the observed broadening at the transition. For 6FDA−TMPDA/azide films, the decrease in T_g is less drastic. The chemical cross-links formed between the poly(azide) and 6FDA−TMPDA restrict the chain movement of the host polyimide and increase its T_g. This partially counteracts the effect of lowering T_g attributed by the poly(azide) phases. A similar broadening of the glass transition for 6FDA−NDA/azide films is observed for 6FDA−TMPDA/azide. DMA was conducted for the pseudo-IPNs

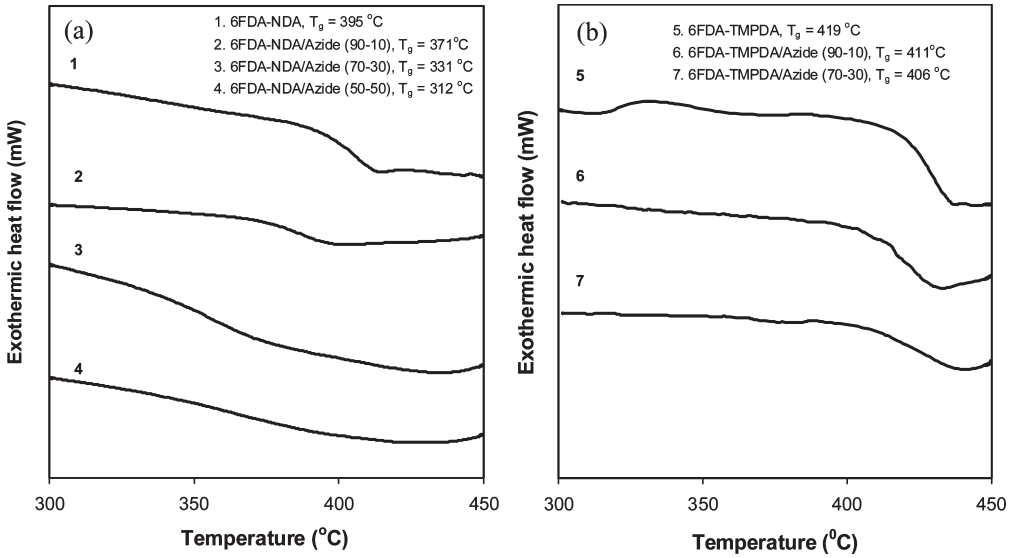

Figure 7. DSC analysis of the (a) 6FDA−NDA/azide and (b) 6FDA−TMPDA/azide films.

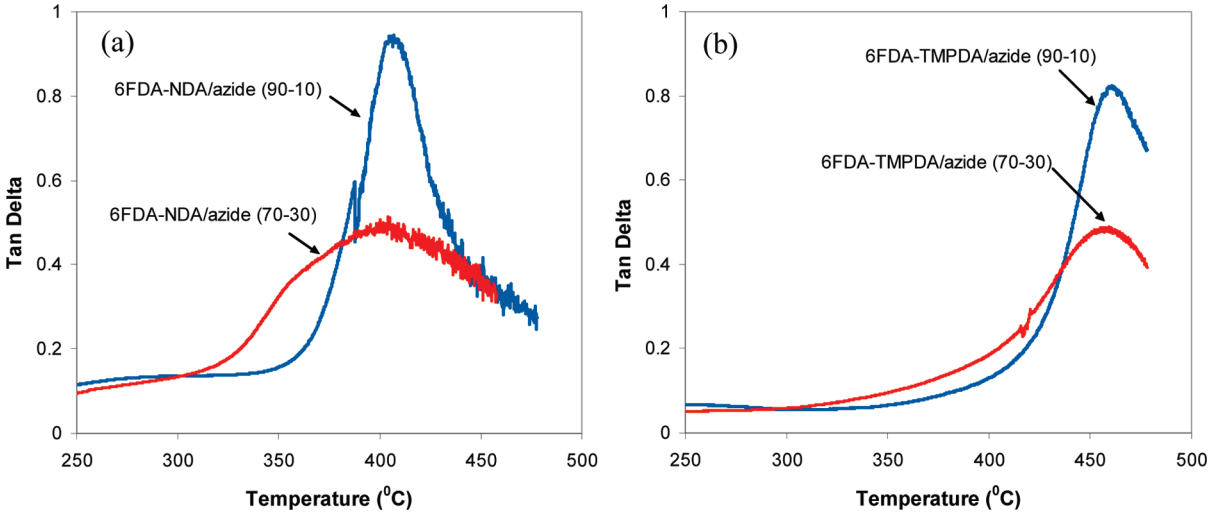

Figure 8. DMA of (a) 6FDA−NDA/azide and (b) 6FDA−TMPDA/azide films.

Table 2. Thermal decomposition properties of 6FDA−polyimide/azide pseudo IPNs

sample	temperature at 5% weight loss (°C)
6FDA−NDA	516.5
6FDA−NDA/azide (90−10)	468.4
6FDA−NDA/azide (70−30)	418.0
6FDA−NDA/azide (50−50)	381.3
6FDA−TMPDA	504.6
6FDA−TMPDA/Azide (90−10)	432.3
6FDA−TMPDA/Azide (70−30)	394.1
poly(azide)	359.8

and the results are shown in Figure 8, parts a and b. The tan δ displays a single local maximum as a function of temperature which further proves the homogeneity of the material.

The thermal degradation properties of the pseudo-IPNs were analyzed and the temperatures at 5% weight loss are summarized in Table 2. The incorporation and polymerization of azide within the polyimide frameworks decrease the thermal stability of the membranes. This is attributed to the lower degradation temperature of the poly(azide) domains. Comparing the decomposition temperatures of the pseudo-IPNs (i.e., 380−470 °C depending on the composition of azide) with other polymers, the thermal properties of the composite materials are not inferior and are sufficient for use in most polymeric membrane-based separations. The derivative weight loss for all the pseudo-IPNs shows two major degradation peaks, one in the range of 300−500 °C and the other between 500 and 700 °C. The former is a due to the decomposition of the azide domains while the latter is attributed to the degradation of the polyimide domains. There is no indication of reaction reversibility for both the pseudo-IPNs at elevated temperatures.

The chain packing of the pseudo-IPNs and the free volume distribution were investigated. Parts a and b of Figure 9 show the results obtained from the XRD analyses of the 6FDA−NDA/azide and 6FDA−TMPDA/azide films. For the 6FDA−NDA/azide films, the addition of azide leads to a marginal decrease in the average *d*-space from 5.7 to 5.5 Å. Moreover, the intensities of the shoulder peaks at $2\theta = 20$ and 26° (corresponding *d*-spaces of 4.4 and 3.4 Å) with respect to

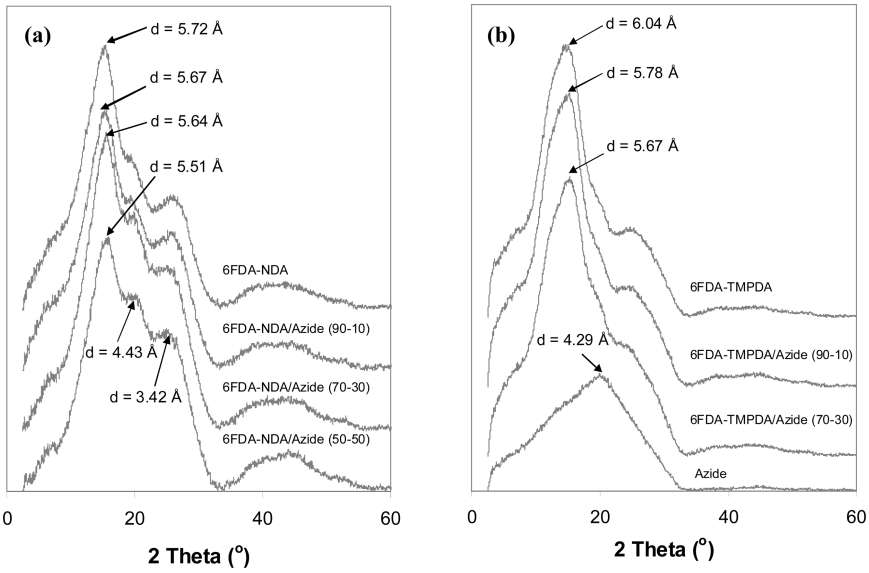

Figure 9. XRD analysis of the (a) 6FDA−NDA/azide and (b) 6FDA−TMPDA/azide films.

Table 3. Positronium Lifetimes, Intensities, Mean Free-Volume Radii and Fractional Free Volume for 6FDA−NDA/Azide and 6FDA−TMPDA/Azide Films

sample	τ_3 (ns)	I_3 (%)	r_3 (Å)	v_{f3} (Å^3)	FFV (%)
6FDA−NDA	2.94 ± 0.02	5.36 ± 0.06	3.60 ± 0.01	195.16 ± 1.67	1.88 ± 0.04
6FDA−NDA/azide (90−10)	2.57 ± 0.03	2.66 ± 0.05	3.33 ± 0.02	154.97 ± 2.36	0.74 ± 0.02
6FDA−NDA/azide (70−30)	2.59 ± 0.05	1.97 ± 0.05	3.35 ± 0.03	157.05 ± 3.70	0.56 ± 0.03
6FDA−NDA/azide (50−50)	2.58 ± 0.04	1.55 ± 0.04	3.34 ± 0.02	155.40 ± 3.40	0.43 ± 0.02
6FDA−TMPDA	2.70 ± 0.02	6.13 ± 0.06	3.42 ± 0.01	168.13 ± 1.56	1.86 ± 0.03
6FDA−TMPDA/azide (90−10)	2.60 ± 0.03	4.43 ± 0.06	3.36 ± 0.01	158.29 ± 2.02	1.26 ± 0.03
6FDA−TMPDA/azide (70−30)	2.47 ± 0.03	3.87 ± 0.06	3.26 ± 0.02	144.57 ± 2.13	1.01 ± 0.03

the prominent amorphous peak show gradual increases at higher azide contents. Similarly, for 6FDA−TMPDA/azide films, the *d*-space changes from 6.0 to 5.7 Å with the incorporation of azide. The addition of azide alters the chain packing of the original host polyimides and densifies the polymer matrix.

The free volumes and free volume distributions of the peudo-IPNs were probed using PALS. The raw data obtained were resolved into three finite lifetime components using the PATFIT program which assumes a Gaussian distribution for the logarithm of the lifetime for each component.[56] The first component is due to the annihilation of parapositronium (p-Ps) ($\tau_1 \approx 0.125$ ns), the second is contributed by the free positrons ($\tau_2 \approx 0.4$ ns) and the last component is attributed to the annihilation of localized orthopositronium (o-Ps) in the polymer free volume ($\tau_3 > 0.5$ ns).[47] Thus, τ_3 is a useful parameter for determining the average cavity size in the polymer and the corresponding intensity, I_3 reflects the quantity of cavities present. The mean free-volume radius (r_3 in Å) can be computed using a semiempirical equation based on a spherical infinite potential well model as shown by eq 7.[47]

$$\tau_3^{-1} = 2\left[1 - \frac{r_3}{r_3+\Delta r} + \frac{1}{2\pi}\sin\left(\frac{2\pi(r_3)}{r_3+\Delta r}\right)\right] \quad (7)$$

where Δr is an empirical constant (1.656 Å) obtained by fitting well-defined cavities with known dimensions (e.g., zeolites). Since the cavities are assumed to be spherical, the mean free volume of a cavity and the relative fractional free volume are given by eqs 8 and 9, respectively.[47]

$$v_{f3} = \frac{4}{3}\pi(r_3)^3 \quad (8)$$

$$\mathrm{FFV} = CI_3 v_{f3}\tau_3 \quad (9)$$

where C is a material-dependent constant (0.001−0.003 for polymers). The positronium lifetimes and intensities, and the calculated free volume radius and FFV are summarized in Table 3.

Generally, the addition of azide to the host polyimides decreases the τ_3 and I_3 values. This means that the formation of a poly(azide) network within the linear polyimide framework leads to smaller cavity sizes and reduces the quantity of free volume. A comparison between the pristine 6FDA−NDA film and the pseudo-IPN with 10 wt % azide shows that the τ_3 decreases from 2.94 to 2.57 ns while the corresponding r_3 changes from 3.60 to 3.33 Å. Further increase in the azide content does not adjust the τ_3 and r_3 values. I_3 which indicates the quantity of free volume, decreases from 5.36 to 1.55% as the azide content in the film increases from 0 to 50 wt %. The corresponding FFV changes from 1.88 to 0.43%. These demonstrate that a small amount of azide is sufficient to fulfill the purpose of altering the free volume cavity size while an overdose of azide merely leads to diminishing free volume with no variation on the mean cavity size. For the 6FDA−TMPDA/azide films, raising the azide content from 0 to 30 wt % steadily decreases the τ_3 and I_3 values. In other words, both the size and quantity of

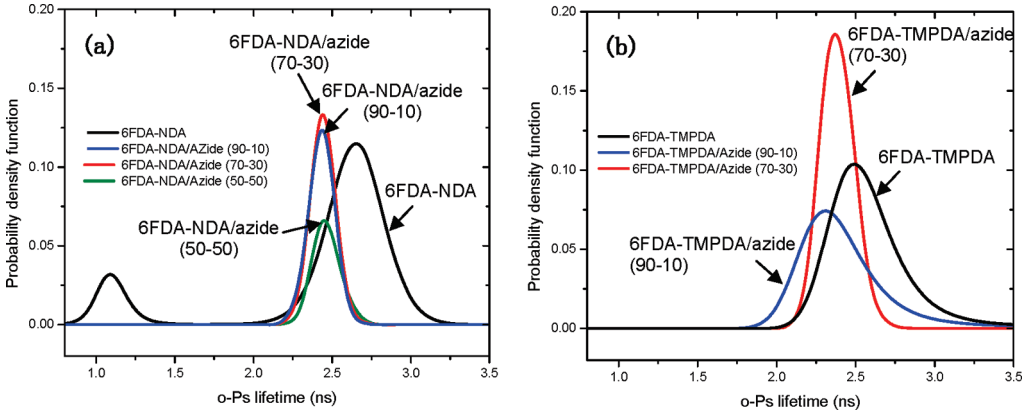

Figure 10. PALS analysis of the (a) 6FDA−NDA/azide and (b) 6FDA−TMPDA/azide films.

Table 4. Pure Gas Permeability of 6FDA−NDA/Azide and 6FDA−TMPDA/Azide Films Tested at 35 °C and 10 atm (Unless Otherwise Stated)[a]

	gas permeability (barrer)						
sample	He	H_2 (3.5 atm)	O_2	N_2	CH_4	CO_2 (3.5 atm)	CO_2
6FDA−NDA	80.2	77.6	8.99	1.74	1.02	42.6	38.0
6FDA−NDA/azide (90−10)	43.9	38.6	3.27	0.54	0.26	14.7	12.9
6FDA−NDA/azide (70−30)	30.2	26.0	1.80	0.28	0.14	7.75	6.61
6FDA−NDA/azide (50−50)	24.4	21.1	1.38	0.20	0.11	5.87	4.99
6FDA−TMPDA	261	358	69.9	19.4	15.5	362	315
6FDA−TMPDA/azide (90−10)	153	186	29.3	7.12	5.29	155	133
6FDA−TMPDA/azide (70−30)	79.4	86.1	9.65	1.97	1.22	44.1	38.6

[a] Barrer = v 1×10^{-10} cm^3 (STP) cm/cm^2 s cmHg =7.5005 $\times10^{-18}$ m^2 s^{-1} Pa^{-1}.

the free volumes diminish gradually in the presence of more poly(azide) domains.

To have a clearer picture of the free volume distribution of the pseudo-IPNs, MELT analysis was utilized and the results are illustrated in Figure 10, parts a and b.[57] The peak between 2 and 3.5 ns is attributed to the o-Ps annihilation in the amorphous region of the polymeric films.[48] Referring to Figure 9a, the incorporation of 10 wt % azide to 6FDA−NDA shifts the peak to the left and a narrower distribution is observed. For 30 and 50 wt % Azide, the positions of the peaks remain essentially the same but the peak intensities decrease. This is in agreement with the trend of constant τ_3 and decreasing I_3 concluded from the PATFIT results. For 6FDA−TMPDA/azide films, the incorporation of 10 wt % azide similarly shifts the peak to the right and a further increment to 30 wt % azide gives rise to a sharper distribution. Therefore, an effective tuning of the free volume cavities of the host polyimides can be achieved via the addition of appropriate amounts of azide monomers.

3.4. Gas Transport Properties and Potential Application in Membrane Gas Separation. The changes in the size and quantity of the cavities, and the free volume distribution of the pseudo-IPNs may be beneficial for the separation of small molecules by polymeric membranes. Therefore, the polyimide/poly(azide) composite films were analyzed for their gas transport properties. The pure gas permeability and ideal gas pair permselectivity of the pseudo-IPNs are shown in Tables 4 and 5, respectively. From Table 4, it can be seen that the gas permeability for both series of pseudo-IPNs decrease in the following order: $P_{He} > P_{H_2} > P_{CO_2} > P_{O_2} > P_{N_2} > P_{CH_4}$. This trend is in accordance to the kinetic diameters of the gases where d_{He} (2.60 Å) < d_{H_2} (2.89 Å) < d_{CO_2} (3.30 Å) < d_{O_2} (3.46 Å) < d_{N_2} (3.64 Å) < d_{CH_4} (3.80 Å). The gas transport properties of the polymeric membranes can be correlated to the free volume and free volume distribution. PALS analyses have shown that the addition of azide decreases the size and quantity of free volume. This consequently reduces the available pathways within the polymeric matrix for gas transport to take place and thus the gas permeability decreases with increasing azide loadings as shown in Table 4. For both series of pseudo-IPNs, the increase in azide content decreases the relative FFV. The natural logarithm of the gas permeability is inversely proportional to the FFV which is in agreement with the exponential relationship between gas permeability and FFV proposed by Alentiev and Yampolski.[58]

One point to highlight here is the gas permeability of the polymeric membrane is dependent on both the mean cavity size (i.e., r_3) and the quantity of free volume (i.e., I_3). PALS analyses utilize positron with a dimension of 1.6 Å to probe the free volume.[48] This means that cavity sizes larger than 1.6 Å are considered in the free volume analysis. However, the cavities with hole size in between 1.6 Å and the kinetic diameter of the gas are inaccessible to the gas molecules and do not contribute to the overall gas transport. From Table 3, the r_3 and relative FFV for 6FDA−NDA are greater than 6FDA−TMPDA but the gas permeability of the latter is more than three times higher than the former. One reason to account for this discrepancy is the inaccessible free volume of 6FDA−NDA possibly makes up a major portion of the total free volume probed by the positrons. Due to the complexity of the o-Ps formation within the polymer membranes, the I_3 value may be influenced by other parameters in addition to the quantity of free volume. In fact, the o-Ps pick-off annihilation intensity depends on the probability of o-Ps formation which is related to the chemical environment in which the o-Ps pickoff occurs. Both 6FDA−NDA and 6FDA−TMPDA consist of electrophilic imide rings but due to the different diamine moiety that constitutes each polyimide, the degree of electrophilicity varies. The difference in

Table 5. Ideal Gas Pair Permselectivity of 6FDA−NDA/Azide and 6FDA−TMPDA/Azide Films

	permselectivity			
sample	O_2/N_2	CO_2/CH_4	H_2/CO_2	H_2/N_2
6FDA−NDA	5.18	37.4	1.82	44.6
6FDA−NDA/azide (90−10)	6.06	49.5	2.63	71.6
6FDA−NDA/azide (70−30)	6.43	47.2	3.35	92.9
6FDA−NDA/azide (50−50)	6.90	45.4	3.60	105
6FDA−TMPDA	3.60	20.3	1.00	18.5
6FDA−TMPDA/azide (90−10)	4.12	25.1	1.20	26.1
6FDA−TMPDA/azide (70−30)	4.90	31.6	1.95	43.7

the electron density affects the probability of forming a positronium i.e. bonding of a trapped positron to a free electron. With these intervening parameters in play, a direct comparison of the relative FFV obtained from PALS analysis for the two host polyimides may not be appropriate. For the pseudo-IPNs, the presence of the poly(azide) similarly changes the chemical environment. Nevertheless, for each series of pseudo-IPNs, the chemical species present are the same i.e. the host polyimide and the poly(azide). Hence, a comparison of the free volume data within each series of pseudo-IPNs is justifiable.

The incorporation of 10 wt % azide to 6FDA−NDA considerably enhances the CO_2/CH_4 selectivity from 37 to 50 which is attributed to the effective tuning of cavity sizes i.e. r_3 changes from 3.6 to 3.3 Å and the free volume distribution becomes narrower. The sharpening of the free volume distribution eliminates the larger cavities where CH_4 transport takes place more favorably. From Table 5, it is clear that further increase in the azide concentration brings about a slight decrease in the CO_2/CH_4 selectivity. The additional azide does not alter the mean cavity size but decreases the quantity of free volume for CO_2 transport i.e. smaller I_3. The decrease in the available free volume impacts CO_2 transport more than CH_4. The addition of azide from 0 to 50 wt % modifies the size and quantity of the free volume effectively, resulting in an increase in H_2/N_2 selectivity from 45 to 105. The improvement in H_2/CO_2 selectivity is not impressive as the transport of CO_2 is not effectively hindered. For O_2/N_2, only a slight increase in selectivity is obtained because of the close kinetic diameters of O_2 and N_2.

For 6FDA−TMPDA/azide interconnected pseudo-IPNs, the increase in the azide content from 0 to 30 wt % leads to a steady increase in the CO_2/CH_4 selectivity as the mean cavity size decreases from 3.4 to 3.3 Å. At a low azide content of 10 wt %, the free volume distribution shifts toward the region of lower cavity sizes while a further increment to 30 wt % azide significantly sharpens the free volume distribution as shown in Figure 10b. Moreover, the formation of chemical cross-links between the 6FDA−TMPDA and poly(azide) phases enhances the chain rigidity of the polymer chains, thereby enhancing the CO_2/CH_4 selectivity. The trends for the remaining gas pairs are similar to the 6FDA−NDA/azide films. As depicted in Figure 11, the CO_2/CH_4 separation performances of the polyimides and the pseudo IPNs display typical trade-off relationship between permeability and permselectivity.

A potential application of the polyimide/poly(azide) pseudo-IPNs is membrane-based natural gas sweetening. Membrane technology is attractive for the industrial purification of natural gas but one major limitation of using polymeric membranes is the tendency for the polymers to swell in the presence of plasticizing components, i.e., CO_2, H_2S, and

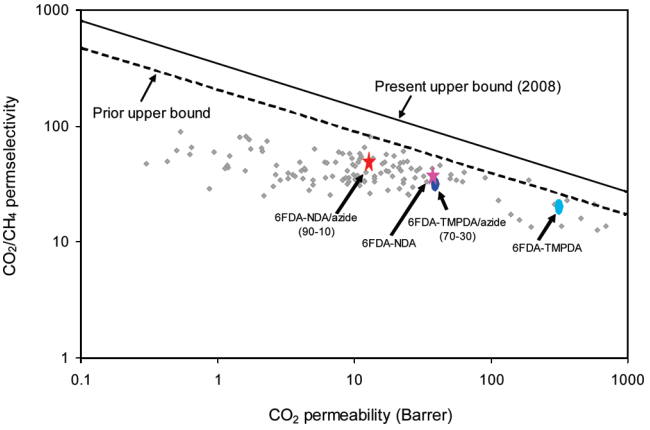

Figure 11. Comparison between the CO_2/CH_4 separation performance of the polyimide/poly(azide) membranes with Robeson's upper bound.

H_2O. Plasticization results in pressure, temperature and time dependency of the membrane separation performance. Thus, polymeric membranes with antiplasticization properties are desirable for reliable separation performance in the long run. In view of these concerns, the CO_2-plasticization behaviors of the pristine polyimides and the respective pseudo-IPNs with the most promising CO_2/CH_4 selectivity were investigated. The CO_2-plasticization curves are depicted in Figure 12, parts a and b. 6FDA−NDA with the highly rigid naphthalene structures shows no sign of CO_2-induced plasticization up to a testing pressure of 30 atm and 6FDA−NDA/azide (90−10) showed similar decline in CO_2 permeability with increasing pressure. 6FDA−TMPDA is more easily swelled by the condensable CO_2 and the onset of CO_2-induced plasticization is at 15 atm. The addition of azide to 6FDA−TMPDA effectively suppresses this undesirable effect i.e. absence of CO_2-induced plasticization up to 30 atm. The formation of denser interconnected pseudo-IPNs restricts the chain movement and enhances the antiplasticization property of the material.

Binary CO_2/CH_4 tests were conducted for the pristine polyimide films and the pseudo-IPN membranes with good ideal permselectivity. A comparison of the gas separation performance of the membranes at different pressures is shown in Table 6. The results obtained from the mixed gas tests are in agreement with the pure gas tests i.e. the addition of azide improves the CO_2/CH_4 permselectivity. Due to the competitive sorption effects rooted from the coexistence of two gas species in the feed stream, the gas permeability obtained from mixed gas tests is lower. As shown in Table 6, 6FDA−TMPDA suffers from severe CO_2-induced plasticization which accounts for the increase in CO_2 permeability and the significant loss of CO_2/CH_4 selectivity at elevated pressures. Conversely, 6FDA−NDA exhibits mild plasticization response where the CO_2 permeability stays relatively constant while the selectivity decreases. The incorporation of azide effectively eliminates the undesirable effects of CO_2-induced plasticization. The CO_2 permeability and CO_2/CH_4 selectivity of 6FDA−TMPDA/azide (70−30) and 6FDA−NDA/azide (90−10) decrease as the pressure increases. This is attributed to the saturation of CO_2 sorption sites at higher pressures.

4. Conclusions and Future Work

The in situ polymerization of azide within rigid polyimide frameworks creates homogeneous pseudo-IPNs with enhanced gas transport properties. The tendency of the nitrenes to react with C−H bonds is a potentially useful way of functionalizing

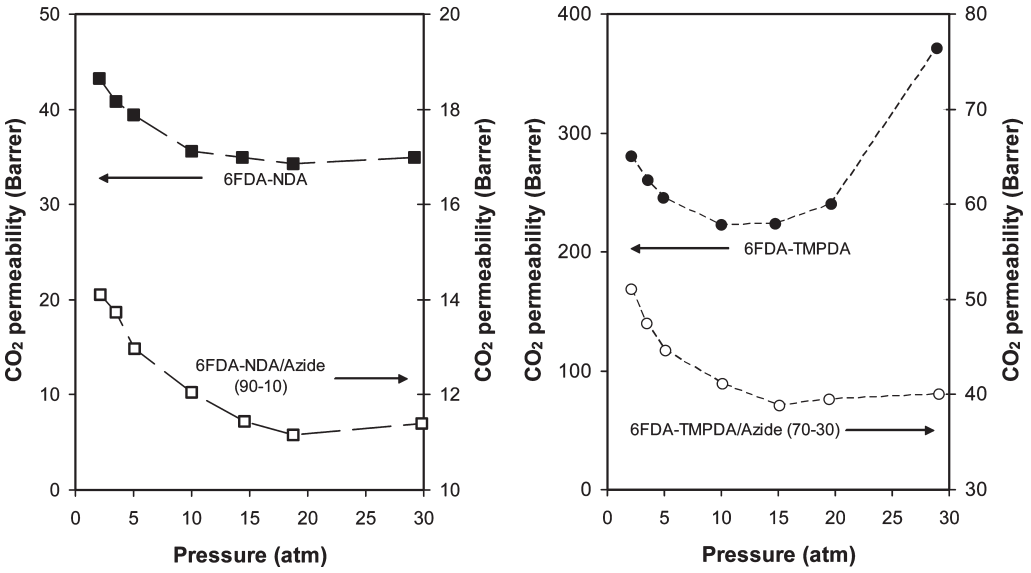

Figure 12. CO_2 plasticization behavior of (a) 6FDA−NDA and 6FDA−NDA/azide (90−10) and (b) 6FDA−TMPDA and 6FDA−TMPDA/azide (70−30) films.

Table 6. CO_2/CH_4 Separation Performance Obtained from Binary Gas Tests at 35 °C[a]

	binary CO_2/CH_4 (90:10) at 10 atm		binary CO_2/CH_4 (90:10) at 20 atm		binary CO_2/CH_4 (90:10) at 30 atm	
sample	P_{CO_2} (barrer)	α_{CO_2/CH_4}	P_{CO_2} (barrer)	α_{CO_2/CH_4}	P_{CO_2} (barrer)	α_{CO_2/CH_4}
6FDA−NDA	25.8	45.9	25.8	41.8	26.0	32.2
6FDA−NDA/azide (90−10)	18.2	56.5	16.2	47.1	12.0	37.1
6FDA−TMPDA	246	24.8	254	18.1	276	9.3
6FDA−TMPDA/azide (70−30)	37.1	32.1	31.7	26.8	28.9	25.4

[a] Barrer = 1×10^{-10} cm^3 (STP) cm/cm^2 s cmHg = 7.5005×10^{-18} m^2 s^{-1} Pa^{-1}.

unactivated C−H bonds that are present in numerous polymers. The incorporation and polymerization of azide within the host polyimide effectively manipulates the cavity size and free volume distribution. The exploration of this synthetic approach on dense flat membranes provides the fundamental understanding of the pseudo-IPNs formation and their physiochemical properties. As a continuation of this study, the future work should be devoted to investigating (1) the feasibility of this approach on asymmetric membranes, (2) the possibility of using other azido-containing monomers for tuning the free volume distribution, and (3) the potential use of this material for other applications.

The applicability of this approach to asymmetric membranes is undeniably challenging due to the complexity of the pseudo-IPN formation coupled with the phase inversion process. The formation of the pseudo-IPN prior to phase inversion may be required if the extractability of the azido-containing monomer by the external coagulant poses a problem. For the spinning of hollow fibers, the preheating of the polymer dope in the syringe pump or within the spinneret leads to partial formation of the pseudo-IPN. This reduces the extractability of the azido-monomers from the extruded fibers during precipitation. To fabricate flat asymmetric membranes, the partial evaporation of the as-cast film at elevated temperatures before immersing into the coagulant bath may be a feasible approach. Instead of using thermal energy, UV light may be utilized for the activation of nitrene reactions to form the psuedo-IPNs. Another possible solution is the use of appropriate coagulant which is a poor solvent for the azido-monomers. The molecular dimensions of the azido-containing monomer greatly influence the cavity size of the resultant pseudo-IPNs. The azide monomer employed in our study has relatively large molecular dimensions and thus there is a limit on the tuning of the free volume distribution. The choice of other azido-containing monomers with smaller dimensions may create pseudo-IPNs that are beneficial for H_2/CO_2 separation. It is also possible to create pseudo-IPNs with multimodal free volume distribution via utilizing appropriate combinations of monomers with different molecular dimensions. Pseudo-IPNs with multimodal free volume distribution may achieve simultaneous increase in both permeability and permselectivity. Due to the nature of the nitrene reactions, amine derivatives are formed which possibly alters the hydrophilicity of the material. Therefore, the polyimide/poly(azide) pseudo IPNs may be useful in pervaporation (e.g., alcohol dehydration) and vapor permeation applications.

Acknowledgment. The authors would like to thank the Singapore National Research Foundation (NRF) for the support on the Competitive Research Programme for the project "Molecular Engineering of Membrane Materials: Research and Technology for Energy Development of Hydrogen, Natural Gas and Syngas" (grant number R-279-000-261-281) and A*Star support for the project "Polymeric Membrane Development for CO_2 Capture from Flue Gas" (Grant No. R-398-000-058-305). Special thanks are dedicated to Professor Maria R. Coleman, Dr. Youchang Xiao, and Dr. Lu Shao for their valuable suggestions to this work.

Note Added after ASAP Publication. This article was published ASAP on August 19, 2009. Modifications have been made to Figures 4 and 10, and Tables 2, 3, and 4. The correct version was published on August 25, 2009.

References and Notes

(1) Xiao, Y.; Low, B. T.; Hosseini, S. S.; Chung, T. S.; Paul, D. R. *Prog. Polym. Sci.* **2009**, *34*, 561–580.
(2) Lemanski, J; Lipscomb, G. *AIChE J.* **1995**, *41*, 2322–2326.
(3) Bhide, B. D.; Stern, S. A. J. *Membr. Sci.* **1993**, *81*, 239–252.
(4) Abetz, V.; Brinkmann, T.; Dijkstra, M.; Ebert, K.; Fritsch, D.; Ohlrogge, K.; Paul, D.; Peinemann, K.-V.; Nunes, S. P.; Scharnagl, N.; Schossig, M. *Adv. Eng. Mater.* **2006**, *8*, 328–358.
(5) Baker, R. W. *Ind. Eng. Chem. Res.* **2002**, *41*, 1393–1411.
(6) Stern, S. A. *J. Membr. Sci.* **1994**, *94*, 1–65.

(7) Lin, H.; Van Wager, E.; Freeman, B. D.; Toy, L. G.; Gupta, R. P. *Science* **2006**, *311*, 639–642.
(8) Kelkar, A. J.; Paul, D. R. J. *Membr. Sci.* **2001**, *181*, 199–212.
(9) Park, H. B.; Jung, C. H.; Lee, Y. M.; Hill, A. J.; Pas, S. J.; Mudie, S. T.; Van Wagner, E.; Freeman, B. D.; Cookson, D. J. *Science* **2007**, *318*, 254–258.
(10) Sroog, C. E. *Prog. Polym. Sci.* **1991**, *16*, 561–694.
(11) Cecopieri-Gómez, M. L.; Palacios-Alquisira, J.; Domínguez, J. M. *J. Membr. Sci.* **2007**, *293*, 53–65.
(12) Coleman, M. R.; Koros, W. J. *J. Membr. Sci.* **1990**, *50*, 285–297.
(13) Wang, Y.-C.; Huang, S.-H.; Hu, C.-C.; Li, C.-L.; Lee, K.-R.; Liaw, D.-J.; Lai, J.-Y. *J. Membr. Sci.* **2005**, *248*, 15–25.
(14) Car, A.; Stropnik, C.; Yave, W.; Peinemann, K.-V. *Adv. Funct. Mater.* **2008**, *18*, 2815–2823.
(15) Patel, N. P.; Spontak, R. J. *Macromolecules* **2004**, *37*, 1394–1402.
(16) Hayes, R. A. US. Patent No. 4,981,497.
(17) Xiao, Y.; Chung, T. S.; Chng, M. L. *Langmuir* **2004**, *20*, 8230–8238.
(18) Shao, L; Liu, L.; Cheng, X. S.; Huang, Y. D.; Ma, J. *J. Membr. Sci.* **2008**, *312*, 174–185.
(19) Low, B. T.; Xiao, Y; Chung, T. S.; Liu, Y. *Macromolecules* **2008**, *41*, 1297–1309.
(20) Powell, C. E.; Duthie, X. J.; Kentish, S. E.; Qiao, G. G.; Stevens, G. F. *J. Membr. Sci.* **2007**, *291*, 199–209.
(21) Wind, J. D.; Paul, D. R.; Koros, W. J. *J. Membr. Sci.* **2004**, *228*, 227–236.
(22) Wind, J. D.; Staudt-Bickel, C.; Paul, D. R.; Koros, W. J. *Macromolecules* **2003**, *36*, 1882–1888.
(23) Omole, I. C.; Miller, S. J.; Koros, W. J. *Macromolecules* **2008**, *41*, 6367–6375.
(24) Kruczek, B.; Matsuura, T. *J. Membr. Sci.* **2000**, *167*, 203–216.
(25) Guiver, M. D.; Robertson, G. P.; Dai, Y.; Bilodeau, F; Kang, Y. S.; Lee, K. J.; Jho, J. Y.; Won, J J. *Polym. Sci. Part A: Polym Chem* **2002**, *40*, 4193–4204.
(26) Ilconich, J. B.; Xu, X.; Coleman, M.; Simpson, P. J. *J. Membr. Sci.* **2003**, *214*, 143–156.
(27) Ruaan, R.-C.; Wu, T.-H.; Chen, S.-H.; Lai, J.-Y. *J. Membr. Sci.* **1998**, *138*, 213–220.
(28) Maeda, Y.; Paul, D. R. *Polymer* **1985**, *26*, 2055–2063.
(29) Muruganandam, N.; Paul, D. R. *J. Membr. Sci.* **1987**, *34*, 185–198.
(30) Bos, A.; Punt, I.; Strathmann, H.; Wessling, M. *AIChE J.* **2001**, *47*, 1088–1093.
(31) Hosseini, S. S; Teoh, M. M.; Chung, T. S. *Polymer* **2008**, *49*, 1594–1603.
(32) Gitsov, I.; Zhu, C. *J. Am. Chem. Soc.* **2003**, *125*, 11228–11234.
(33) Meseguer Dueñas, J. M.; Torres Escuriola, D.; Gallego Ferrer, G.; Monleón Pradas, M.; Gómez Ribelles, J. L.; Pissis, P.; Kyritsis, A. *Macromolecules* **2001**, *34*, 5525–5534.
(34) Pandit, S. B.; Kulkarni, S. S.; Nadkarni, V. M. *Macromolecules* **1994**, *27*, 4595–4604.
(35) Tamai, T.; Imagawa, A.; Tran-Cong, Q. *Macromolecules* **1994**, *27*, 7486–7489.
(36) Leger, C.; Nguyen, Q. T.; Neel, J.; Streicher, C. *Macromolecules* **1995**, *28*, 143–151.
(37) Wang, M.; Pramoda, K. P.; Goh, S. H. *Chem. Mater.* **2004**, *16*, 3452–3456.
(38) Izuka, A.; Winter, H. H.; Hashimoto, T. *Macromolecules* **1997**, *30*, 6158–6165.
(39) Kurdi, J.; Kumar, A. *J. Membr. Sci.* **2006**, *280*, 234–244.
(40) Chng, M. L.; Xiao, Y.; Chung, T.-S.; Torrida, M.; Tamai, S. *Carbon* **2009**, *47*, 1857–1866.
(41) Bos, A.; Punt, I. G. M.; Wessling, M.; Strathmann, H. *J. Polym. Sci., Part B: Polym. Phys.* **1998**, *36*, 1547–1556.
(42) Lee, D. S.; Kang, W. K.; An, J. H.; Kim, S. C. *J. Membr. Sci.* **1992**, *75*, 15–27.
(43) Kurdi, J.; Kumar, A. *Polymer* **2005**, *46*, 6910–6922.
(44) Saimani, S.; Kumar, A. *J. Appl. Polym. Sci.* **2008**, *110*, 3606–3615.
(45) Jean, Y. C.; Yuan, J. P.; Liu, J.; Deng, Q.; Yang, H. *J. Polym. Sci., Part B: Polym. Phys.* **1995**, *33*, 2365–2371.
(46) Hu, C.-C.; Lee, K.-R.; Ruaan, R.-C.; Jean, Y. C.; Lai, J.-Y. *J. Membr. Sci.* **2006**, *274*, 192–199.
(47) Lue, S. J.; Lee, D.-T.; Chen, J.-Y.; Chiu, C.-H.; Hu, C.-C. *J. Membr. Sci.* **2008**, *325*, 831–839.
(48) Cheng, M.-L.; Sun, Y.-M.; Chen, H.; Jean, Y. C. *Polymer* **2009**, *50*, 1957–1964.
(49) Jean, Y. C.; Hong, X.; Liu, J.; Huang, C. M.; Cao, H.; Chung, C. Y.; Dai, G. H.; Cheng, K. L.; Yang, H. *J. Radioanal. Nucl. Chem.* **1996**, *210*, 513–524.
(50) Shao, L.; Chung, T. S.; Goh, S. H.; Pramoda, K. P. *J. Membr. Sci.* **2005**, *256*, 46–56.
(51) Moody, C. J.; Whitham, G. H. *Reactive intermediates*; Oxford University Press: New York, 1992.
(52) Socrates, G. *Infrared and Raman characteristic group frequencies: tables and charts*, 3rd ed.; Wiley: New York, 2000.
(53) Morison, R. T.; Boyd, R. N. *Organic Chemistry*, 6th ed.; Prentice Hall: Upper Saddle River, NJ, 1992.
(54) Kelman, S. D.; Rowe, B. W.; Bielawski, C. W.; Pas, S. J.; Hill, A. J.; Paul, D. R.; Freeman, B. D. *J. Membr. Sci.* **2008**, *320*, 123–134.
(55) Shao, L.; Samseth, J.; Hagg, M.-B. *J. Membr. Sci.* **2009**, *326*, 285–292.
(56) Kirkegaard, P.; Eldrup, M.; Mogensen, O. E.; Pedersen, N. J. *Comput. Phys. Commun.* **1981**, *23*, 307–335.
(57) Shukla, A.; Hoffmann, L.; Manuel, A. A.; Peter, M. *Mater. Sci. Forum* **1997**, *255*, 233–237.
(58) Alentiev, A. Y.; Yampolskii, Y. P. *J. Membr. Sci.* **2002**, *206*, 291–306.